Current Collapse Suppression by Gate Field-Plate in AlGaN/GaN HEMTs Md.

Current Collapse Suppression by Gate Field-Plate in AlGaN/GaN HEMTs

Md. Tanvir Hasan, *Student Member, IEEE*, Takashi Asano, Hirokuni Tokuda, and Masaaki Kuzuhara, *Fellow, IEEE*

***Abstract*—Current collapse measurements have been performed for AlGaN/GaN HEMTs having identical breakdown voltages but with different field plate (FP) lengths. The results indicated that applying more positive on-state gate biases resulted in pronounced recovery in the dynamic on-resistance for the FP device, whereas no gate-bias effects were observed for the device without FP. The mechanism responsible for the reduced current collapse by FP is proposed, in which the key role is played during on-state by the quick field-effect recovery of partial channel depletion caused by electron trapping at AlGaN surface states between gate and drain.**

***Index Terms*—AlGaN/GaN HEMT, field plate, on-resistance, current collapse.**

I. Introduction

An AlGaN/GaN-based high-electron-mobility transistor (HEMT) is considered as an excellent candidate for future power devices due to its high breakdown voltage, high saturation drain current, and low on-resistance (R_{on}) [1], [2]. However, increased dynamic R_{on} by current collapse is regarded as one of the most critical issues to be solved for actual power-switching applications [3]-[4]. Various techniques have been reported as an effective approach to suppress current collapse, such as surface passivation [5], surface charge control with GaN cap layer [6], and field plate (FP) structure [7]-[10]. Saito *et al.* reported that the FP approach enhanced the breakdown voltage and hence suppressed the increase of dynamic R_{on} due to relaxation of electric field crowding at the gate edge in the drain side [9]. Brannick *et al.* reported by their computer simulation that FP was effective to reduce electron trapping by limiting tunneling injection of electrons into surface traps located in the gate-to-drain region [10]. Evidently, no experimental evidences have been identified to date with respect to the effect of FP on the dynamic switching performance of AlGaN/GaN HEMTs.

In this letter, we report measurement results of dynamic R_{on} for a series of AlGaN/GaN HEMTs with essentially the same breakdown voltage but with different FP lengths. Dramatic reduction in current collapse is presented for the FP device, in which trap-induced increase in the gate-to-drain access resistance is quickly recovered by the field effect of positively biased FP electrode.

Manuscript received March 26, 2013.

M. T. Hasan, T. Asano, H. Tokuda and M. Kuzuhara are with the Graduate School of Engineering, University of Fukui, Bunkyo 3-9-1, Fukui 910-8507, Japan (email: tan_vir_bd@yahoo.com, kuzuhara@fuee.u-fukui.ac.jp).

II. Device Fabrication

The epitaxial structure used in this work was grown by MOCVD on a 4H-SiC substrate. It consists of a 500-nm GaN channel, and a 25-nm $Al_{0.25}Ga_{0.75}N$ barrier. Hall-effect measurements showed a two-dimensional electron gas (2DEG) density of 1.01×10^{13} cm^{-2} and an electron mobility of 1500 cm^2/Vs.

HEMT device fabrication began with mesa isolation using BCl_3/Cl_2-based inductively coupled plasma reactive ion etching. Source and drain ohmic contacts were formed by e-beam evaporation of Ti/Al/Mo/Au metal stacks, followed by rapid thermal annealing at 850 °C for 30 s in a N_2 atmosphere. A contact resistance of 0.34 Ωmm was measured. Devices were then passivated with a 200-nm sputter-deposited SiN film. The gate window was opened by dry etching of the SiN film, followed by Schottky gate and FP formation with Ni/Au. The gate length, gate-to-source distance, and gate width were fixed at 3, 3, and 100 μm, respectively.

III. Device Characteristics and Discussion

Essentially the same dc characteristics have been measured for devices with and without FP. With a gate-to-drain distance (L_{GD}) of 10 μm, the maximum drain current defined at V_{GS}=1 V was 500 mA/mm and the gate-to-drain leakage current was 10^{-7} A/mm measured at a bias voltage of 200V.

Fig.1 shows static R_{on} and breakdown voltage as a function of L_{GD} for devices without FP. The off-state source-to-drain breakdown voltage was defined at a drain current of 0.1 mA/mm. During the measurements, the back side of SiC substrate was kept floating. Almost the same dependence of static R_{on} and breakdown voltage on L_{GD} has been measured for devices with different FP length (L_{FP}) of 1, 3, and 5 μm. Here, to avoid possible breakdown between FP and drain, L_{FP} of 1 μm was only tested for the device with L_{GD}=5 μm. The static R_{on} and the breakdown voltage were in the range of 9.5-10.7 Ωmm and 700-740 V, respectively, for devices with L_{GD}=10 μm. The linear increase in the breakdown voltage, as shown in Fig. 1, suggests that the horizontal electric field would not be crowded

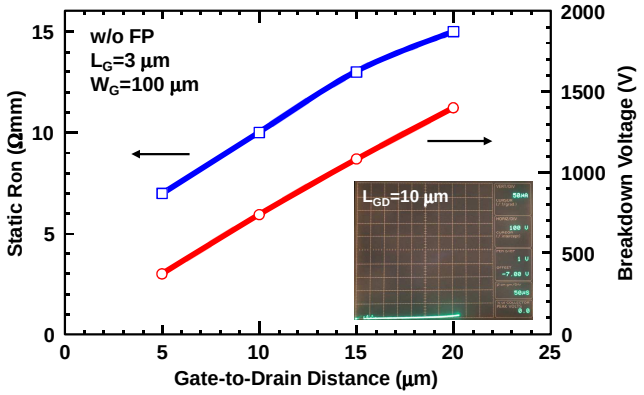

Fig. 1. Static on-resistance and breakdown voltage as a function of gate-to-drain distance (L_{GD}) for AlGaN/GaN HEMTs without field plate. Inset shows breakdown characteristics for the device with L_{GD}=10 μm.

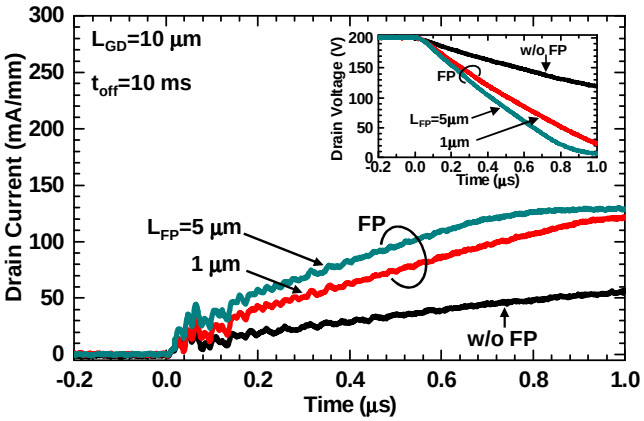

Fig. 2. Transient drain current of AlGaN/GaN HEMTs with and without FP. Pulsed mode is operated with 15 kΩ load line with off-state drain bias voltage of 200 V. Inset shows transient drain voltage.

near the gate edge. The virtual gate model [3] is a qualitative explanation for the increasing tendency of breakdown voltage with L_{GD}, but does not account for the linear increase with L_{GD} that we have observed between devices with different L_{FP}. Such linear increase in the breakdown voltage, as shown in Fig. 1, would be more reasonably explained if we assume a constant electric field distribution between gate and drain, even though direct experimental verification of field distribution has not yet been successfully made. Instead, our 2-dimensional device simulation (data not shown) suggested that uniform field distribution could be established when the surface negative charge was distributed uniformly with a sheet density that was balanced with the positive polarization charge at the AlGaN/GaN interface. The importance of balanced negative and positive polarization charges for establishing uniform field distribution has been proposed as a concept of natural super junction [11]. More work is needed to verify the possibility of forming uniform field distribution during off states by the presence of balanced negative and positive polarization charges on the front and back surfaces of AlGaN.

Characterization of dynamic R_{on} was carried out by on-wafer pulsed measurements, where the gate voltage was switched from off-state (V_{GS}=-5 V, below the threshold voltage of -3.7 V) to on-state (V_{GS}=1 V), while applying a drain bias voltage (V_{DS})

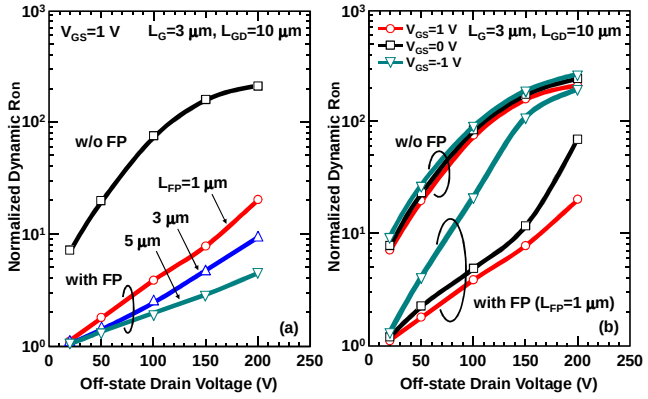

Fig. 3. Normalized dynamic on-resistance as a function of off-state drain bias voltage for AlGaN/GaN HEMTs with and without FP. (a) Dependence of L_{FP} and (b) dependence of V_{GS}.

up to 200 V. The load resistance (R_L) was connected in series with the tested device and was adjusted so that R_{on} was reasonably measured in the linear region, i.e., below 1/4 of the maximum drain current. The on-state duration time (t_{on}) and the off-state duration time (t_{off}) were fixed at 1 μs and 10 ms, respectively. The transient output current was measured by a current probe (LeCroy CP030). Fig. 2 shows measured time-dependent waveforms of the drain current and the drain voltage (insert) of devices with and without FP. A constant R_L of 15 kΩ was used at V_{DS}=200 V. Although the drain current waveform exhibited an oscillatory response in the early stage (up to 200 ns), our setup was able to stably measure the drain current response with a time constant of more than 300 ns. The measurement accuracy of on-state current was about ±0.03 mA and that of voltage was less than ±0.1 V. The device without FP exhibited seriously degraded drain current response with a long time constant (more than 1 ms), while the drain current recovery was much faster for the FP device. The dynamic R_{on} measured at t_{on}=1 μs was as large as 2220 Ωmm for the device without FP, while that for the FP device (L_{FP}=5 μm) was only 45 Ωmm. More interestingly, the drain current recovery became faster as L_{FP} was increased, indicating that the gate-FP structure with reasonably long L_{FP} is effective to reduce dynamic R_{on}.

To represent the magnitude of current collapse quantitatively, we have defined the normalized dynamic R_{on}, where the R_{on} value measured at t_{on}=1 μs was normalized by its static value. For devices without FP, the normalized dynamic R_{on} was gradually increased from 190 to 320 with increasing L_{GD} from 5 to 20 μm. Fig. 3 (a) shows the normalized dynamic R_{on} as a function of off-state V_{DS} with V_{GS}=1 V. It is obvious that the dynamic R_{on} increases with increasing V_{DS}. Note that the normalized dynamic R_{on} for the FP device is lowered by 1 or 2 orders of magnitude as compared to the device without FP, indicating that only reducing the exposed-access distance (i.e., L_{GD}-L_{FP}) is not enough for significant current collapse reduction. These results demonstrate a primary advantage of FP to suppress current collapse. To our knowledge, this is the first report showing experimental evidence of current collapse suppression by using gate FP, where the dynamic R_{on} was compared among devices with essentially the same breakdown

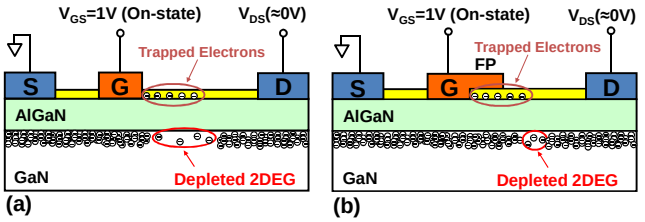

Fig. 4. Schematic diagrams of on-state device operation for AlGaN/GaN HEMTs (a) without FP and (b) with FP.

voltages. Fig. 3 (b) shows normalized dynamic R_{on} as a function of V_{DS} with different V_{GS}. For the device without FP, the normalized dynamic R_{on} was increased with increasing V_{DS}, approaching more than 200 at V_{DS}=200 V. This behavior was almost independent of the on-state V_{GS} between -1 and +1 V. On the other hand, for the FP device, V_{GS} dependence was clearly observed, where normalized dynamic R_{on} was significantly reduced by increasing on-state V_{GS} from negative to positive values due to generation of capacitively-induced additional channel charge (on the order of 10^{11} cm^{-2}) in the early stage of on states (up to t_{on}=1 μs). Note that the normalized dynamic R_{on} of the FP device with V_{GS}=-1 V is approaching to that for the device without FP, indicating that FP electrode becomes less effective on dynamic R_{on} when on-state V_{GS} was set at negative values under high V_{DS} conditions.

Fig. 4 shows the schematic diagram of device operation under on states for AlGaN/GaN HEMTs with and without FP. During off state with V_{GS}=-5 V, both devices are considered essentially the same, where channel 2DEG electrons are fully depleted under the gate. Due to strong reverse electric fields between gate and drain during off states, electrons are injected from the gate edge as leakage currents and are assumed to be trapped at the AlGaN/SiN interface. Hence, higher drain bias voltages lead to enhancement of trapped electrons [12]. Those trapped electrons contribute to partly deplete the channel 2DEG electrons near the gate edge in the drain side. Next the gate voltage is switched to on state (V_{GS}=1 V), resulting in quick generation of electron accumulation under the gate. However, emission of captured electrons does not occur within a short period of time (i.e., less than 1 μs). Hence it takes rather a long time before steady-state condition is reached for the device without FP (see Fig. 4 (a)). This is the main reason for causing the current collapse. On the other hand, the situation for the FP device is quite different, as shown in Fig. 4 (b). Since the AlGaN surface near the gate is covered with FP, the partial depletion of 2DEG electrons can be instantly recovered by the field effect of the positively-biased FP electrode. Therefore, the recovery of channel electrons is much faster for the FP device, leading to more enhanced improvements in dynamic performance during on states with more positive gate biases, as shown in Fig. 3 (b).

IV. Conclusion

We have studied the effect of gate FP on current collapse for a series of AlGaN/GaN HEMTs having essentially the same breakdown voltage but with different FP lengths. By applying a more positive on-state gate bias voltage, pronounced recovery in the dynamic on-resistance was observed for the FP device, whereas no significant gate-bias effects were observed for the device without FP. The mechanism responsible for the improved current collapse was proposed, where field-effect charge control by FP resulted in the quick recovery of partial channel depletion in the gate-to-drain access region.

Acknowledgment

This work was performed as a part of the project named "Development of Nitride-based Semiconductor Crystal Substrate and Epitaxial Growth Technology" by NEDO.

References

[1] S. C. Binari, K. Ikossi, J. A. Roussos, W. Kruppa, D. Park, H. B. Dietrich, D. D. Koleske, A. E. Wickenden, and R. L. Henry, “Trapping effects and microwave power performance in AlGaN/GaN HEMTs,” IEEE Trans. Electron Devices, vol. 48, no. 3, pp. 465–471, Mar. 2001.

[2] R. Chu, A. Corrion, M. Chen, R. Li, D. Wong, D. Zehnder, B. Hughes, and K. Boutros, “1200-V normally off GaN-on-Si field-effect transistors with low dynamic ON-resistance,” IEEE Electron Device Lett., vol. 32, no. 5, pp. 632–634, May 2011.

[3] R. Vetury, N. Q. Zhang, S. Keller, and U. K. Mishra, “The impact of surface states on the DC and RF characteristics of AlGaN/GaN HFETs,” IEEE Trans. Electron Devices, vol. 48, no. 3, pp. 560–566, Mar. 2001.

[4] W. Saito, T. Nitta, Y. Kakiuchi, Y. Saito, K. Tsuda, I. Omura, and M. Yamaguchi, “Suppression of dynamic On-resistance increase and gate charge measurements in high-voltage GaN-HEMTs with optimized field-plate structure,” IEEE Trans. Electron Devices, vol. 54, no. 8, pp. 1825–1830, Aug. 2007.

[5] B. M. Green, K. K. Chu, E. M. Chumbes, J. A. Smart, J. R. Shealy, and L. F. Eastman, “The effect of surface passivation on the microwave characteristics of undoped AlGaN/GaN HEMTs,” IEEE Electron Device Lett., vol. 21, no. 6, pp. 268–270, Jun. 2000.

[6] T. Kikkawa et al, “Surface charge controlled AlGaN/ GaN-power HEFT without current collapse and g_m,” in IEDM Tech. Dig., 2001, pp. 25.4.1 - 25.4.4.

[7] Y. Ando, Y. Okamoto, H. Miyamoto, T. Nakayama, T. Inoue, and M. Kuzuhara, “10-W/mm AlGaN–GaN HFET with a field modulating plate,” IEEE Electron Device Lett., vol. 24, no. 5, pp. 289–291, May 2003.

[8] Y. Wu, A. Saxler, M. Moore, R. P. Smith, S. Sheppard, P. M. Chavarkar, T. Wisleder, U. K. Mishra, and P. Parikh, “30W/mm GaN HEMTs by field plate optimization,” IEEE Electron Device Lett., vol. 25, no. 3, pp. 117–119, Mar. 2004.

[9] W. Saito, Y. Kakiuchi, T. Nitta, Y. Saito, T. Noda, H. Fujimoto, A. Yoshioka, T. Ohno, and M. Yamaguchi, “Field-plate structure dependence of current collapse phenomena in high-voltage GaN-HEMTs,” IEEE Electron Device Lett., vol. 31, no. 7, pp. 659–661, Jul. 2010.

[10] A. Brannick, N. A. Zakhleniuk, B. K. Ridley, J. R. Shealy, W. J. Schaff, and L. F. Eastman, “Influence of field plate on the transient operation of the AlGaN/GaN HEMT,” IEEE Electron Device Lett., vol. 30, no. 5, pp. 436–438, May 2009.

[11] H. Ishida, D. Shibata, M. Yanagihara, Y. Uemoto, H. Matsuo, T. Ueda, T. Tanaka, and D. Ueda, “Unlimited high breakdown voltage by natural super junction of polarized semiconductor,” IEEE Electron Device Lett., vol. 29, no. 10, pp. 1087–1089, Oct. 2008.

[12] Z. Tang, S. Huang, Q. Jiang, S. Liu, C. Liu, and K. J. Chen, “High-voltage (600-V) low-leakage low-current-collapse AlGaN/GaN HEMTs with AlN/SiN_x passivation,” IEEE Electron Device Lett., vol. 34, no. 3, pp. 366–368, Mar. 2013.